Compact 2D nonlinear photonic crystal source of beamlike path entangled photons

E. Megidish,[1,*] A. Halevy,[1] H. S. Eisenberg,[1] A. Ganany-Padowicz,[2] N. Habshoosh,[2] and A. Arie[2]

[1]*Racah Institute of Physics, Hebrew University of Jerusalem, Jerusalem 91904, Israel*

[2]*School of Electrical Engineering, Fleischman Faculty of Engineering, Tel Aviv University, Tel Aviv 69978, Israel*

[*]*hagaie@huji.ac.il*

Abstract: We demonstrate a method to generate entangled photons with controlled spatial shape by parametric down conversion (PDC) in a 2D nonlinear crystal. A compact and novel crystal source was designed and fabricated, generating directly path entangled photons without the use of additional beam-splitters. This crystal supports two PDC processes, emitting biphotons into two beamlike modes simultaneously. Two coherent path entangled amplitudes of biphotons were created and their interference observed. Our method enables the generation of entangled photons with controlled spatial, spectral and polarization properties.

OCIS codes: (190.4410) Nonlinear optics, parametric processes; (270.0270) Quantum optics.

References and links

1. P. G. Kwiat, K. Mattle, H. Weinfurter, A. Zeilinger, A. V. Sergienko, and Y. Shih, "New high intensity source of polarization-entangled photon pairs," Phys. Rev. Lett. **75**, 4337–4341 (1995).
2. J. A. Armstrong, N. Bloembergen, J. Ducuing, and P. S. Pershan, "Interactions between light waves in a nonlinear dielectric," Phys. Rev. **127**, 1918–1939 (1962).
3. M. M. Fejer, G. A. Magel, D. H. Jundt, and R. L. Byer, "Quasi-phase-matched second harmonic generation: tuning and tolerances," IEEE J. Quantum Electron. **28**, 2631–2654 (1992).
4. T. Ellenbogen, N. Voloch-Bloch, A. Ganany-Padowicz, and A. Arie, "Nonlinear generation and manipulation of Airy beams," Nat. Photonics **3**, 395–398 (2009).
5. N. Voloch-Bloch, K. Shemer, A. Shapira, R. Shiloh, I. Juwiler, and A. Arie, "Twisting light by nonlinear photonic crystals," Phys. Rev. Lett. **108**, 233902 (2012).
6. J. P. Torres, A. Alexandrescu, S. Carrasco, and L. Torner, "Quasi-phase-matching engineering for spatial control of entangled two-photon states," Opt. Lett. **29**, 376–378 (2004).
7. H. Y. Leng, X. Q. Yu, Y. X. Gong, P. Xu, Z. D. Xie, H. Jin, C. Zhang, and S. N. Zhu, "On-chip steering of entangled photons in nonlinear photonic crystals," Nat. Commun. **2**, 429 (2011).
8. R. Shiloh and A. Arie, "Spectral and temporal holograms with nonlinear optics," Opt. Lett. **37**, 3591–3593 (2012).
9. R. Lifshitz, A. Arie, and A. Bahabad, "Photonic quasicrystals for nonlinear optical frequency conversion," Phys. Rev. Lett. **95**, 133901 (2005).
10. S. N. Zhu, Y. Y Zhu, and N. B Ming, "Quasi-phase-matched third-harmonic generation in a quasi-periodic optical superlattice," Science **278**, 843–846 (1997).
11. V. Berger, "Nonlinear photonic crystals," Phys. Rev. Lett. **81**, 4136–4139 (1998).
12. N. Broderick, G. Ross, H. Offerhaus, D. Richardson, and D. Hanna, "Hexagonally poled lithium niobate: a two-dimensional nonlinear photonic crystal," Phys. Rev. Lett. **84**, 4345–4348 (2000).
13. J. J. Bollinger, W. M. Itano, D. J. Wineland, and D. J. Heinzen, "Optimal frequency measurements with maximally correlated states," Phys. Rev. A **54**, R4649–R4652 (1996).

#183517 - $15.00 USD Received 16 Jan 2013; revised 24 Feb 2013; accepted 24 Feb 2013; published 11 Mar 2013

14. J. G. Rarity, P. R. Tapster, E. Jakeman, T. Larchuk, R. A. Campos, and M. C. Teich, "Two-photon interference in a Mach-Zehnder interferometer," Phys. Rev. Lett. **65**, 1348–1351 (1990).
15. C. K. Hong, Z. Y. Ou, and L. Mandel, "Measurement of subpicosecond time intervals between two photons by interference," Phys. Rev. Lett. **59**, 2044–2046 (1987).
16. M. W. Mitchell, J. S. Lundeen, and A. M. Steinberg, "Super-resolving phase measurements with a multiphoton entangled state," Nature (London) **429**, 161–164 (2004).
17. T. Nagata, R. Okamoto, J. L. OBrien, K. Sasaki, and S. Takeuchi, "Beating the standard quantum limit with four-entangled photons," Science **316**, 726–729 (2007).
18. I. Afek, O. Ambar, and Y. Silberberg, "High-NOON states by mixing quantum and classical light," Science **328**, 879–881 (2010).
19. C. E. Kuklewicz, M. Fiorentino, G. Messin, F. N. C. Wong, and J. H. Shapiro, "High-flux source of polarization entangled photons from a periodically poled $KTiOPO_4$ parametric down-converter," Phys. Rev. A **69**, 013807 (2004).
20. T. Kim, M. Fiorentino, and F. N. C. Wong, "Phase-stable source of polarization-entangled photons using a polarization Sagnac interferometer," Phys. Rev. A **73**, 012316 (2006).
21. Y.-H. Kim, "Quantum interference with beamlike type-II spontaneous parametric down-conversion," Phys. Rev. A **68**, 013804 (2003).
22. A. Arie, N. Habshoosh, and A. Bahabad, "Quasi phase matching in two-dimensional nonlinear photonic crystals," Opt. Quant. Electron. **39**, 361–375 (2007).
23. Y.-X. Gong, P. Xu, Y. F. Bai, J. Yang, H. Y. Leng, Z. D. Xie, and S. N. Zhu, "Multiphoton path-entanglement generation by concurrent parametric down-conversion in a single $\chi^{(2)}$ nonlinear photonic crystal," Phys. Rev. A **86**, 023835 (2012).
24. J. Jacobson, G. Björk, I. Chuang, and Y. Yamamoto, "Photonic de Broglie Waves," Phys. Rev. Lett. **74**, 4835–4838 (1995).
25. I. Dolev, A. Ganany-Padowicz, O. Gayer, A. Arie, J. Mangin, and G. Gadret, "Linear and nonlinear optical properties of MgO:$LiTaO_3$," Appl. Phys. B **96**, 423–432 (2009).
26. M. Yamada, N. Nada, M. Saitoh, and K. Watanabe, "First-order quasi-phase matched $LiNbO_3$ waveguide periodically poled by applying an external field for efficient blue second-harmonic generation," Appl. Phys. Lett. **62**, 435–436 (1992).
27. D. Branning, S. Bhandari, and M. Beck, "Low-cost coincidence-counting electronics for undergraduate quantum optics," Am. J. Phys. **77**, 667–670 (2009).
28. K. Edamatsu, R. Shimizu, and T. Itoh, "Measurement of the photonic de broglie wavelength of entangled photon pairs generated by spontaneous parametric down-conversion," Phys. Rev. Lett. **89**, 213601 (2002).
29. M. J. Holland and K. Burnett, "Interferometric detection of optical phase shifts at the Heisenberg limit," Phys. Rev. Lett. **71**, 1355–1358 (1993).
30. Y.-X. Gong, P. Xu, J. Shi, L. Chen, X. Q. Yu, P. Xue, and S. N. Zhu, "Generation of polarization-entangled photon pairs via concurrent spontaneous parametric downconversions in a single $\chi^{(2)}$ nonlinear photonic crystal," Opt. Lett. **37**, 4374–4376 (2012).
31. H. Jin, P. Xu, X. W. Luo, H. Y. Leng, Y. X. Gong, and S. N. Zhu, "Compact engineering of path entangled sources from a monolithic quadratic nonlinear photonic crystal," http://arxiv.org/abs/1302.0162.

1. Introduction

Entangled photonic states are commonly generated using the nonlinear process of optical parametric down-conversion (PDC) [1]. In PDC, a single pump photon is converted into two lower energy photons in a quadratic nonlinear crystal. As the pump photon and the down-converted photons are of different wavelengths, phase-matching (PM) conditions have to be fulfilled in the form of momentum and energy conservation. As a result, the down-converted photons are highly correlated in many degrees of freedom. The PM conditions can be fulfilled in several ways, such as angle and temperature tuning in birefringent crystals and with the quasi phase matching (QPM) method, using periodically or aperiodically poled crystals [2, 3].

The QPM technique involves a spatial modulation of the second-order nonlinearity of the material. As a result, the PM criteria must be satisfied while taking into account the modulated nonlinearity. The PM condition in *k*-space (the reciprocal lattice) is therefore

$$\overline{k}_{2w} - \overline{k}_{w_1} - \overline{k}_{w_2} = \overline{G}_n \,, \tag{1}$$

where $\overline{k}_{2\omega}$ is the momentum of the pump, $\overline{k}_{\omega_i}$ the momentum of the down-converted photons, and $\overline{G}_n$ is a reciprocal lattice vector of the nonlinear crystal. The modulation vector and the

#183517 - $15.00 USD Received 16 Jan 2013; revised 24 Feb 2013; accepted 24 Feb 2013; published 11 Mar 2013

material dispersion properties determine which wavelengths satisfy the PM conditions. Additionally, other properties of the generated beams can be controlled by careful tuning of the modulation, such as their shape [4,5], focusing [6,7], and spectral properties [8]. At first, QPM was realized by one dimensional periodic modulation, but later more sophisticated modulation patterns appeared, such as quasiperiodic modulation [9,10] and two-dimensional periodic modulation [11,12]. These patterns provide a larger variety of reciprocal lattice vectors, hence offering more possibilities for phase matching. When the nonlinear coefficient is periodically modulated along two directions, a two-dimensional nonlinear photonic crystal (NPC) is formed. This NPC supports modulation vectors $\overline{G}_{m,n} = mG_x\hat{x} + nG_y\hat{y}$ with two degrees of freedom, such that PM can be fulfilled in several directions and for different wavelengths.

Entanglement can be realized between various degrees of freedom of the photons. In this work, we focus on entanglement between the number of photons and their path. Such states are superpositions of two N-photon amplitudes, in which all the photons are in one of two possible optical modes or in the other. When the two modes are interfered, oscillations that are N times faster than the wavelength are observed. These states have been shown to exceed the classical limit of measurement accuracy and can be used to reach the quantum Heisenberg limit [13]. Path entangled states were demonstrated by Hong-Ou-Mandel (HOM) bunching photons at a balanced beam-splitter (BS) [14,15], combining a few photons statistically with BSs [16], post-selection of appropriate amplitudes [17], and by combining classical and nonclassical light beams at a BS [18].

Ideally, the PDC process should generate the path entangled states directly into easy to collect beamlike modes. However, in many cases, owing to the rotational symmetry of the nonlinear process, the down converted photons are generated along cones of light [1]. This severely limits the collection efficiency of the entangled photons. An alternative method is to generate the entangled photons in two collinear counter-propagating directions [19,20]. This scheme can provide high efficiency, but requires pumping the nonlinear crystal simultaneously along two counter-propagating directions, filtering of the collinear pump beams, and an interferometric setup for combining the two counter-propagating down-converted photons. Another alternative uses two type-II crystals to generate non-collinear beamlike polarization entangled photons [21]. None of these schemes generates path entangled states directly.

2. Theoretical background

In this work, we demonstrate a path-entangled state that is generated from a two-dimensional periodically poled NPC [22]. This scheme, which was recently proposed theoretically [23], overcomes the limitations of existing methods by controlling the spatial properties of the down-converted photons [6]. The two biphoton states are directly generated into well defined non-collinear beamlike modes, using a single pump beam. The reciprocal lattice of the 2D NPC supports two processes. Thus, a pump photon can split into two down-converted photons that are in either one of two coherent well-defined spatial modes [see Fig. 1(a)]. The two-photon state is

$$|\psi^{\varphi}\rangle = \frac{1}{\sqrt{2}}(|2,0\rangle + e^{2i\varphi}|0,2\rangle), \tag{2}$$

where $|a,b\rangle$ is a two-mode Fock state with a photons in one mode and b in the other. The angle φ is a controllable relative phase between the two modes. The accumulated phase between the two amplitudes is twice this angle due to the two-photon effective de-Broglie wavelength [24]. The control of the PM condition through the crystal temperature affects the photons' mode shape and their overall collection efficiency. The phase-matched process is for the d_{zzz} element of the quadratic nonlinear tensor, and thus the pump photon and both down-converted photons

#183517 - $15.00 USD Received 16 Jan 2013; revised 24 Feb 2013; accepted 24 Feb 2013; published 11 Mar 2013

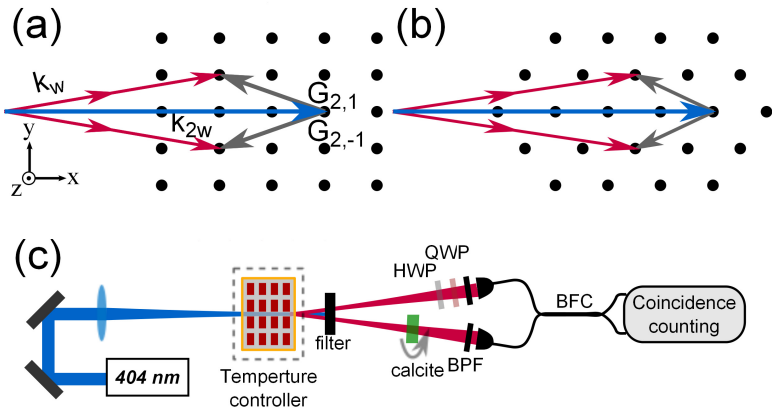

Fig. 1. (a) A reciprocal lattice representation of the momenta involved in the down-conversion processes in the crystal. (b) An alternative possible design that avoids the $G_{2,0}$ circle. (c) The experimental setup (see main text for details).

are all extraordinarily polarized. The reciprocal vector elements in our configuration are

$$\begin{aligned} mG_x &= |\bar{k}_{2w}| - (|\bar{k}_{w_1}| + |\bar{k}_{w_1}|)\cos(\theta), \\ nG_y &= (|\bar{k}_{w_1}| + |\bar{k}_{w_1}|)\sin(\theta). \end{aligned} \tag{3}$$

3. Crystal design and fabrication

The NPC periods were calculated for a stoichiometric $LiTaO_3$ (SLT) crystal [25], where an angle of 0.8° between the pump and the down-converted photons inside the crystal was chosen. For degenerated down-conversion process using 404 nm pump photons, we found $\Lambda_x = 3.2\,\mu$m and $\Lambda_y = 13.46\,\mu$m for m=n=1. In order to avoid a modulation period which is hard to fabricate, we chose m=2, n=1 such that the x period is $\Lambda_x = 6.4\,\mu$m.

For designing our poling pattern we assume a circular motif [22] in each lattice point, i.e., the second order nonlinear coefficient is inverted in circular areas that are centered on each one of the lattice point. The radius R of the circle determines the Fourier coefficient at each spatial frequency and therefore the efficiency of the process. In order to avoid overlap we limit the radius to be less than half of the period. Since this is a rectangular lattice, according to [22] the Fourier coefficient is given by

$$G^x_{m,n} = \frac{2R}{\sqrt{(n\Lambda_x)^2 + (m\Lambda_y)^2}} J_1[2\pi R\sqrt{(\frac{m}{\Lambda_x})^2 + (\frac{n}{\Lambda_y})^2}]. \tag{4}$$

The optimal result is obtained for a motif with a radius of $2.7\,\mu m$, and the Fourier coefficient in this case is 0.087. A 0.5% Mg-doped SLT was poled by electric-field poling. The crystal dimensions were $0.5 \times 13 \times 15$ mm. The inverted domain structure was created by applying an electrical field through patterned electrodes on the crystal surface [26]. High-voltage pulses were applied to the polar crystal surfaces using a computer-controlled system, by limiting the pulse duration at a given current and driving voltage level while monitoring the current and charge transfer. The total switching charge required for complete poling was $60\,\mu$C/cm^2, which was done with an electric field of 3 KV/mm at room temperature. Under these conditions, the maximal current density that we obtained was $25\,\mu$A/cm^2. It should be noted that when one uses small size of motif on the mask (typically less than $5\,\mu$m), it is difficult to control the

#183517 - $15.00 USD Received 16 Jan 2013; revised 24 Feb 2013; accepted 24 Feb 2013; published 11 Mar 2013

exact shape and size of the inverted domains. To overcome this limitation we use a multi-grating design, with different sizes and shapes of the motif on the mask. The good quality of the realized structure can be seen in the inset of Fig. 2. Two gratings have square motifs ($2.4\times 2.4\,\mu$m and $5.5\times 5.5\,\mu$m), and two other gratings have rectangular domains ($5.5\times 6.73\,\mu$m and $2.4\times 6.73\,\mu$m). The inverted domains exhibited nearly circular shape when the square motif was used, and an oval shape when the rectangular motif was used. Each rectangular lattice was poled on an area of $3\times 13\,\text{mm}^2$.

4. Experimental setup and results

A narrow line width diode laser with 35 mW and at a wavelength of 404 nm pumps a two-dimensionally poled stoichiometric $LiTaO_3$ crystal whose temperature is controlled and stabilized within $\pm 0.05^\circ$C [see Fig. 1(c)]. After passing through the 13 mm long crystal, the pump light is filtered out using a dichroic mirror and a long-pass filter. The 808 nm down-converted photons are further filtered by a 3 nm wide bandpass filter (BPF) and spatially filtered by coupling them into single mode fibers. A half-wave plate (HWP) and a quarter-wave plate (QWP) before the fiber coupling of one of the two paths are used to restore the interference between the two paths, which is lost due to the random polarization rotations in the two fibers. The relative phase between the paths is controlled by rotating a 1 mm calcite in one of them. After the two paths are combined at a balanced fiber coupler (BFC), they are coupled into two single photon detectors. The two paths coincidence count rate is detected within a 7 ns window [27].

The angular spread of the down-converted photons was measured using a cooled CCD camera placed after the pump block filter and the narrow bandpass filter. The working condition was searched by tuning the relative angle between the pump and the input facet, and the crystal temperature. These angle and temperature values were set such that the two down-converted modes were generated symmetrically into beamlike modes. For our sample, such beam shape for the $G_{2,1}$ and $G_{2,-1}$ modes was achieved at a crystal temperature of $61.00\pm 0.05^\circ$C, as presented in Fig. 2 by the two filled circles. At lower temperatures, the difference between the refractive indices of the pump and the down-converted photons is smaller, the PM condition is not fulfilled, and no photons are emitted into these modes. On the other hand, when the crystal temperature is increased above this working point, the beamlike PM pattern changes into cones, and its projection on the camera is in the form of circles of increasing radius.

In order to observe the two-photon interference between the two down-converted modes, first the coupling of each mode has to be optimized. When blocking one mode before it is coupled into the fiber, the coupling of the second mode into its respective fiber is optimized through the two detectors' coincidence rate. Similarly, the coupling of the first mode is optimized when the second mode is blocked. Each of these two coincidence rates were about 1000 per second for a pump power of 35 mW. The detection of pairs of photons from each of the modes is not sufficient, as an incoherent mixture of two photons in one of the two modes would still show the same results. In order to demonstrate the presence of coherence between the two process, as in the state of Eq. (2), they are combined at the BFC. The ideal state of Eq. (2) is transformed by the BFC to

$$|\psi'\rangle=\frac{1}{2}(1-e^{2i\varphi})|\psi^{\frac{\pi}{2}}\rangle+\frac{1}{2}(1+e^{2i\varphi})|1,1\rangle\,. \tag{5}$$

When the relative phase between the two paths is scanned, the state oscillates at double the phase between the state $|\psi^{\frac{\pi}{2}}\rangle$ of both photons at a single mode, and the state where their is a single photon in each of the modes. When $\varphi=\pi/2$ or $3\pi/2$, the crystal generated output is an eigenstate of the BFC operation. When $\varphi=0$ or π, the two photons undergo a process which is the inverse of the HOM bunching [15], resulting in the $|1,1\rangle$ anti-bunched state.

Clearly, an additional process is present in the form of a large circle around the pump beam,

#183517 - $15.00 USD Received 16 Jan 2013; revised 24 Feb 2013; accepted 24 Feb 2013; published 11 Mar 2013

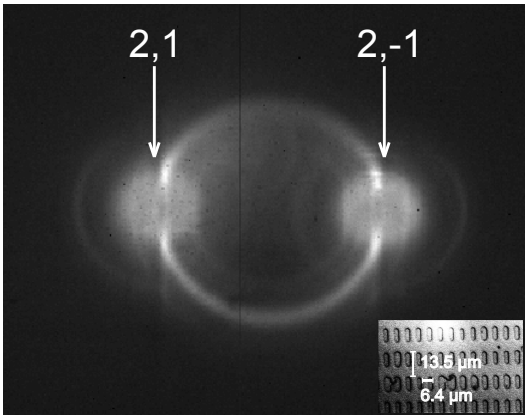

Fig. 2. A picture of the down-converted photons through a 3 nm bandpass filter centered at 808 nm. It was taken using a cooled sensitive camera placed after the pump filter [see Fig. 1(c)]. Inset: an optical microscope picture of the NPC.

overlapping with the two signal beams (Fig. 2). This unwanted process is a result of one down-converted photon emitted along one beam while the other is emitted along the other beam. The crystal PM vector for this process is $G_{2,0}$. The number of events collected from this unwanted process is measured as coincidence events between the two modes. The ratio between the events produced by this unwanted process and the desired $G_{2,\pm1}$ processes is 15%. Although our results are not affected considerably by this process, we note that a non-rectangular reciprocal lattice such as suggested in Fig. 1(b) will eliminate this process, as no reciprocal vector lays at the middle point between the two participating vectors. There are also three weak circles in the picture that we attribute to other possible nonlinear processes.

We measured the single (one photon from either one of the BS ports) and the coincidence counts (two photons exit the BS into different ports) while changing one of the optical path lengths by rotating the 1 mm calcite crystal (see Fig. 1). The single counts show no dependence to the delay changes whereas quantum interference is observed in the coincidence counts [28]. Because two photons are accumulating phase together, the total phase between the two terms of $|\psi^{\varphi}\rangle$ is doubled. This coincidence corresponds to the anti-bunched term of $|\psi'\rangle$. The observed oscillations with a visibility of 72 ± 1% are presented in Fig. 3(b). The oscillation period is half the wavelength of each of the photons, commonly regarded as super-resolution [29].

The non-perfect visibility is attributed to four causes. The fiber coupler has a weak wavelength dependence, resulting in $45/55$% imbalance at the working wavelength. Secondly, there is inaccuracy in the polarization matching of both modes at the BFC, resulting in distinguishability between the two modes. Additionally, the second order term, describing two pump photons that split into four down-converted photons within the coherence time, reduces the visibility. In order to evaluate the second order term effect, we measured the number of pairs created in one path as a function of the pump power. Deviation from a linear dependence indicates the presence of higher order terms. We observed that 10% of the pairs for a 35 mW pump power were created from high order events, and estimate the total effect on the visibility to be a reduction of ~ 7%. Lastly, the anti-bunched pairs from the $G_{2,0}$ circle affect the visibility. Ideally, they do not contribute to the coincidence detection, regardless of the applied φ phase [15].

#183517 - $15.00 USD Received 16 Jan 2013; revised 24 Feb 2013; accepted 24 Feb 2013; published 11 Mar 2013

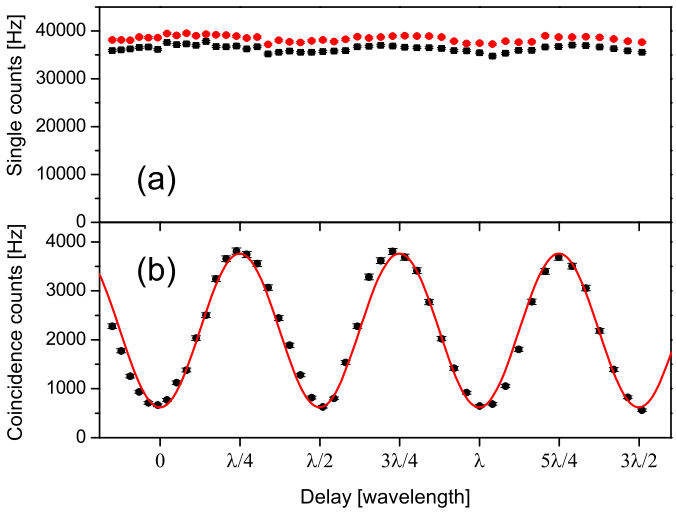

Fig. 3. (a) Single counts of the left (red circles) or right (black squares) port of the BS. No dependence on the relative delay between the two paths is observed. (b) Coincidence counts as a function of the relative delay between the two paths. Interference pattern in the coincidence counts is observed with a contrast of $72 \pm 1\%$. The interference period is half of the photons' wavelength. Error bars are calculated assuming Poissonian noise statistics.

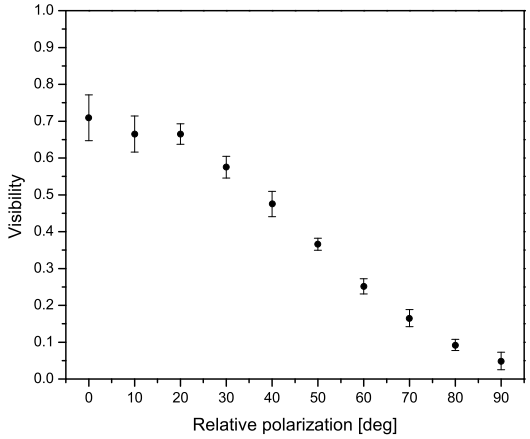

Fig. 4. The interference visibility as a function of the relative polarization rotation between the two paths. At zero angle the two paths are indistinguishable at the BFC and the visibility is maximal. When the polarization of only one path is rotated, distinguishability is introduced and the interference contrast decreases.

Practically, the imbalance of the fiber coupler can generate a constant background signal to the coincidence interference. For the parameters of our experiment, we calculated this background to reduce the visibility by 5%.

The two-photon interference requires complete indistinguishability between the photons in both paths. For the beam combining, spatial overlap is achieved by using a single-mode BFC. Temporal indistinguishability can be determined by the amount of spectral filtering. In our experiment, the pump laser has a coherence time of about 100 ns, which is much longer than the 300 fs coherence time imposed by the 3 nm filters. Therefore, temporal indistinguishability

#183517 - $15.00 USD Received 16 Jan 2013; revised 24 Feb 2013; accepted 24 Feb 2013; published 11 Mar 2013

is not a problem. Polarization difference between the two paths is another degree of freedom that can contribute to distinguishability. As it is easily controlled using the wave plates, it is possible to verify that the interference is between the two spatial modes and not between two polarization modes. We measured the interference visibility while gradually rotating the photon's polarization on one path using a HWP (see Fig. 4). With no rotation, the polarizations of both paths match, and interference is observed. When a relative rotation between the two paths is applied, distinguishability is introduced and the interference decreases. At 90°, there is non-vanishing visibility of about 5%, which is attributed to some elliptical polarization mismatch. As stated above, this also affects the maximal observed visibility.

5. Conclusions

In conclusion, we have demonstrated a method to control the spatial properties of entangled down-converted photons. Two-photon path entangled states were generated from a two-dimensional periodically poled nonlinear crystal. Bunching on a beam splitter is not required as the states are emitted directly from the source. The two paths of the generated state were combined at a fiber coupler and quantum amplitude oscillations with a doubled phase sensitivity were observed. This source demonstrates the ability to simultaneously phase-match more than one quantum process in such two-dimensional crystals. This method can be further extended for generating entangled photons with controlled spatial, spectral and polarization properties. For example, polarization entangled photons can be created using a slightly different scheme in which the same crystal is pumped with *y*-polarized pump, thereby generating pairs of orthogonally polarized photons through the d_{yzy} process [30]. After the submission of this work, a similar independent result was submitted to the Arxiv [31].

Acknowledgments

The authors thank the Israeli Ministry of Science for supporting this work under Project 3-3445, and the Israel Science Foundation for supporting this work under Grants 774/09 and 546/10.

#183517 - $15.00 USD Received 16 Jan 2013; revised 24 Feb 2013; accepted 24 Feb 2013; published 11 Mar 2013